Quantitative measurement of radiation pressure on a microcantilever in ambient environment

Dakang Ma,[1,2] Joseph L. Garrett,[2,3] and Jeremy N. Munday[1,2,a)]
[1]*Department of Electrical and Computer Engineering, University of Maryland, College Park, Maryland 20742, USA*
[2]*Institute for Research in Electronics and Applied Physics, University of Maryland, College Park, Maryland 20742, USA*
[3]*Department of Physics, University of Maryland, College Park, Maryland 20742, USA*

(Received 26 January 2015; accepted 21 February 2015; published online 6 March 2015)

Light reflected off a material or absorbed within it exerts radiation pressure through the transfer of momentum. Micro/nano-mechanical transducers have become sensitive enough that radiation pressure can influence these systems. However, photothermal effects often accompany and overwhelm the radiation pressure, complicating its measurement. In this letter, we investigate the radiation force on an uncoated silicon nitride microcantilever in ambient conditions. We identify and separate the radiation pressure and photothermal forces through an analysis of the cantilever's frequency response. Further, by working in a regime where radiation pressure is dominant, we are able to accurately measure the radiation pressure. Experimental results are compared to theory and found to agree within the measured and calculated uncertainties. © *2015 AIP Publishing LLC*.
[http://dx.doi.org/10.1063/1.4914003]

Maxwell predicted that light is capable of imparting momentum on an object based on his wave-theory of electromagnetism.[1] An equivalent approach can also be used in terms of transmitted/reflected/absorbed photon fluxes.[2] When a photon is reflected or absorbed by an object, there is a transfer of momentum, which results in an applied pressure. The force exerted on an object in free space due to a photon flux at normal incidence is given by[3]

$$F_{rp} = (2R + A)P/c, \tag{1}$$

where F_{rp} is the photon "radiation pressure" force, P is the total incident power, c is the vacuum speed of light, and R and A are the reflection and absorption coefficients resulting from light incident on the object. Though a century old discovery, radiation pressure continues to be of interest to many research areas, such as active cooling of mechanical resonators in cavity optomechanics,[4–7] cantilever spring constant calibration,[8] laser power measurement,[9] enhanced radiation force in a microwave resonant unit,[10] etc. There has also recently been renewed interest in the Abraham-Minkowski controversy, which considers the magnitude of the photon momentum within a material and the partitioning of electromagnetic and mechanical momentum in dielectric systems.[11–14]

Quantitative measurements of radiation pressure in micromechanical systems are often obscured by photothermal effects.[3,5,15,16] Compared with macroscopic resonators, microscopic mechanical resonators have much shorter thermal time constants, ranging from tens of milliseconds to tens of nanoseconds.[4,5,15] In order to mitigate photothermal effects, previous experiments required complex resonator designs consisting of highly reflective multilayer stacks deposited onto large customized cantilevers,[8] micro-scale transfer of a mirror onto a microcantilever,[4] and attachment of a gold mass to a cantilever to increase the thermal time constant.[17] Earlier experiments used a two-laser actuation technique and showed the dominance of radiation pressure on uncoated cantilevers,[2,18] but they lacked accurate quantitative agreement with theory. Further, most measurements are performed in vacuum to avoid radiometric effects,[19] which limit their applicability in micro-scale technologies that operate under ambient conditions. Here, we show an accurate measurement of radiation pressure in an ambient environment on an uncoated silicon nitride microcantilever. We estimate the photothermal contribution to the total measured force, identify the bending direction of the cantilever, and compare experimental results with theoretical calculations, finding agreement within the calculated errors.

The apparatus used for measuring the radiation pressure consists of a modified atomic force microscope (AFM), shown in Fig. 1. We modified the system (Asylum Research, Cypher) by introducing a second laser source ($\lambda = 660$ nm) into the optical path and by focusing the light on the backside of the

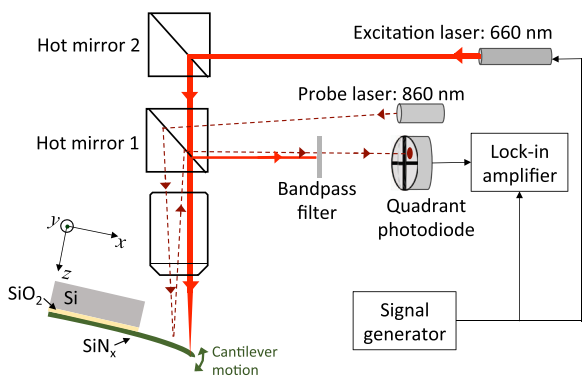

FIG. 1. Experimental setup for measuring the radiation pressure. An external laser (660 nm) is used to excite oscillation of the SiN_x cantilever, and a probe laser beam (860 nm) is used to detect the cantilever motion.

a)Email: jnmunday@umd.edu

cantilever through the same objective (20×) as the probe laser. The focused spot size is estimated to be ~6 μm from the full-width-at-half-max of the beam's Gaussian profile. This laser is driven by a sinusoidal reference signal from a lock-in amplifier and is used to excite the cantilever. The cantilever deflection is detected by a split-quadrant photodetector using the optical lever method, and the amplitude and phase of the signal are determined by the lock-in amplifier. An uncoated rectangular silicon nitride (SiN_x) cantilever (Bruker, MLCT-O10, uncoated) is used in the experiment to reduce photothermal effects caused by photon absorption. It lacks absorption throughout the visible spectrum and is free from bimorphic bending effects found with coated cantilevers.

The radiation pressure induced bending can be distinguished from photothermal bending by its frequency response and bending direction. While radiation pressure is independent of modulation frequency, photothermal bending is not, due to its finite thermal relaxation time. The total effective photothermal force $F_0^{pt}(\omega)$ has a low pass frequency response of the form[4]

$$F_0^{pt}(\omega) = F_0^{pt}(0)/(1 + i\omega\tau), \tag{2}$$

where ω is the laser driving frequency, and τ is the photothermal characteristic time constant. While the origin of the photothermal response is difficult to determine in materials with little absorption (e.g., SiN_x), the photothermal bending in our experiment is likely due to the difference in thermal expansion coefficients between the cantilever and the substrate chip, which is most pronounced when illumination occurs near the base of the cantilever. Although the suspended cantilever is made of silicon nitride only, the base of the cantilever sits atop a silicon oxide layer on a silicon chip (Fig. 1). In this geometry, the cantilever bends towards the silicon substrate when heated,[20] which corresponds to an upward bending in our setup, opposite to that of the radiation pressure.

To determine the forces exerted on the cantilever, we measure the magnitude and phase of the cantilever oscillation under sinusoidal external laser excitation whose modulation frequency is swept across the fundamental resonance frequency of the cantilever. Under this sinusoidal excitation, the force on cantilever has the harmonic form $F(t) = \mathrm{Re}[F_0(\omega)e^{i\omega t}]$. The measured amplitude and phase are then combined to form a complex amplitude phasor, which is fit to a modified damped harmonic oscillator model incorporating the contribution from the radiation pressure and photothermal effects, given by

$$A(\omega) = \frac{A_{rp} + A_{pt}(0)/(1 + i\omega\tau)}{1 - (\omega/\omega_1)^2 + i\omega/(\omega_1 Q)}, \tag{3}$$

where ω is the driving frequency, ω_1 is cantilever's fundamental resonance frequency, and A_{rp} and $A_{pt}(0)$ are the amplitudes of the cantilever displacement at the free end due to the radiation force and the effective photothermal force (i.e., the effective bending force resulting from photothermal bending) at zero-frequency, respectively. Positive values of A_{rp} and $A_{pt}(0)$ indicate a downward bending, while negative values indicate an upward bending according to our coordinates (Fig. 1).

The dominant driving mechanism (radiation pressure or photothermal) depends on the position of cantilever excitation. By controlling the laser excitation position along the longitudinal direction of the cantilever, we determine the frequency response of the cantilever at each position (Fig. 2). The data are fit to Eq. (3) to determine the parameters describing the cantilever's response (Table I). When excited near the base, the cantilever displays a large vibration amplitude, which increases at low frequencies driven by the photothermal effects. For excitation near the free end of the cantilever, radiation pressure dominates at excitation frequencies above a few kHz. This is because the radiation pressure generates a larger total bending moment when it's farther away from the pivot point. On the other hand, photothermal effects are more effective when heating is closer to the pivot point.[21]

The phase signal in our experiments can also indicate different driving mechanisms. The radiation pressure causes a downward deflection of the cantilever (positive) when

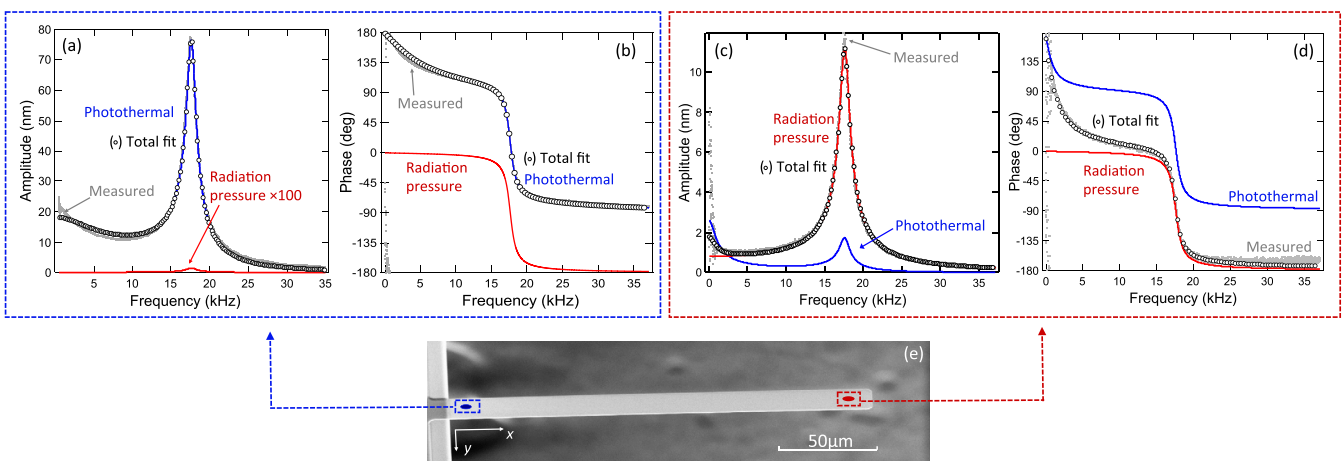

FIG. 2. Frequency response of the cantilever under external illumination near the base ((a) and (b)) and near the free end ((c) and (d)). When the excitation position x_0 is near base ($x_0 = 5\ \mu$m) of the cantilever, the amplitude (a) and phase (b) of the response are dominated by the photothermal component (note: the radiation pressure component is too small to affect the total fit and is estimated from (c) and (d). For excitation near the free end ($x_0 = 185\ \mu$m), the amplitude (c) and phase (d) of the response are dominated by the radiation pressure. (e) An SEM image of the cantilever and excitation positions (the x-axis is defined along the longitudinal direction of the cantilever, the y-axis is along the width, and the origin is at base of the cantilever).

TABLE I. Fitted photothermal and radiation pressure amplitudes at zero frequency and the corresponding thermal time constants from Eq. (3) for excitation near the base and near the free end of the cantilever. The error indicates the 95% confidence intervals of the fitting process. Note: The value of A_{rp} near the base is estimated from the measured value of A_{rp} near the free end, because the contribution of the radiation pressure to the total bending amplitude cannot be resolved by the fitting procedure when illumination is near the pivot point of the cantilever.

	A_{rp} (nm)	$A_{pt}(0)$ (nm)	τ (μs)	f_0 (Hz)	Q
Near free end	-0.813 ± 0.002	2.53 ± 0.05	186 ± 4	$17\,632 \pm 1$	13.59 ± 0.04
Near base	-1×10^{-4}	18.7 ± 0.1	31.1 ± 0.3	$17\,663 \pm 3$	14.78 ± 0.07

illuminated from above, in phase with the excitation signal at dc and lags 90° at resonance (resulting in a phase of −90°). On the other hand, the effective photothermal force causes an upward bending (negative), so the phase signal is 180° at dc and lags more than 90° and at most 180° at resonance, depending on the thermal constant of the low-pass behavior (resulting in 0°–90°). In our measurement, when exciting near the free end, the phase at resonance is approximately −80°, indicating that radiation pressure is dominant but when exciting near the base, the phase at resonance is approximately 20°, indicating that photothermal bending is dominant.

In order to measure the radiation pressure, we focus our attention on the situation where the laser excitation is near the free end ($x_0 = 185\mu m$, where x_0 is the distance from the base). The total measured force is given by

$$F_{0,measure}(\omega) = A(\omega)\left[1 - (\omega/\omega_1)^2 + i\omega/(\omega_1 Q)\right]k_1\frac{1}{\gamma}, \quad (4)$$

where k_1 is the spring constant of the fundamental mode determined by the Sader method,[22,23] and γ is the distributed force correction factor that takes into account the fact that the forces are not point forces exerted at the end of the cantilever $x = L$ (see below). The fitted radiation force and effective photothermal force can be determined, respectfully, from Eqs. (3) and (4) as

$$F^{rp}_{0,fit} = A_{rp}k_1\frac{1}{\gamma} \quad (5)$$

and

$$F^{pt}_{0,fit}(\omega) = \frac{A_{pt}(0)}{(1 + i\omega\tau)}k_1\frac{1}{\gamma}. \quad (6)$$

The distributed force correction factor γ is calculated as the ratio of the cantilever oscillation amplitude generated by a Gaussian distributed pressure at $x = x_0$ with total force F_0 to that generated by a point force F_0 at $x = L$

$$\gamma = \frac{\int_0^L f_{Gauss}(x)\varphi_1(x)dx}{\int_0^L F_0\delta(x-L)\varphi_1(x)dx} = B\frac{\int_0^L e^{-2(x-x_0)^2/w_0^2}\varphi_1(x)dx}{\varphi_1(L)}$$
$$\approx 0.862, \quad (7)$$

where $f_{Gauss}(x)$ is the force per unit length in the longitudinal direction for the Gaussian distributed pressure, $\varphi_1(x)$ is the normalized eigenfunction of the cantilever's fundamental mode,[24,25] w_0 is the beam waist of laser spot, W is the width of the cantilever, and $B = \sqrt{2/\pi}erf(W/\sqrt{2}w_0)/w_0$.

A clear distinction can be made between photothermal and radiation pressure effects for laser excitation rates above a few kHz (Fig. 3). At low frequencies, the effective photothermal force is larger but decays to about 10% of radiation pressure force at the resonance frequency (17.632 kHz). Furthermore, because the two forces are nearly 90° out of phase at resonance frequency, when adding in quadrature, the effective photothermal force accounts for less than 1% of the total amplitude at resonance. Therefore the radiation pressure is the dominant driving force for cantilever resonance.

The measured radiation pressure force agrees with the calculated values from Eq. (1) (Fig. 4). To determine the expected radiation force, we use measured values for the laser power and reflectivity from the cantilever. The reflectivity coefficient, R, is determined from a measurement of the transmitted power through the cantilever, T, as $R = 1 - T$. We have taken the absorption in the cantilever to be approximately zero because the absorption coefficient for SiN_x is much smaller than the reflection and transmission coefficients at 660 nm. The shaded area in Fig. 4 shows the uncertainty in the calculated force based on the uncertainty in the laser power. The error bars on the experimental data result from the

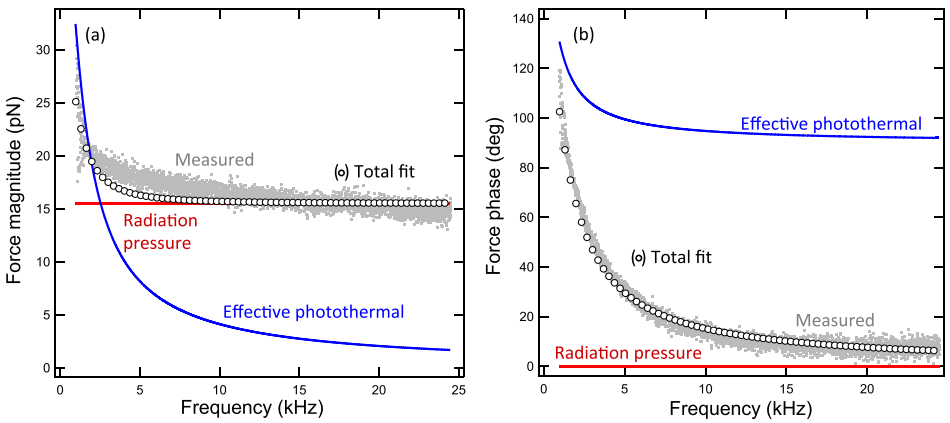

FIG. 3. Determination of force components (radiation pressure and effective photothermal) under sinusoidal illumination (9.32 mW at $\lambda = 660$ nm). The amplitude and phase of the experimental data are simultaneously fit to Eq. (3) and applied to Eqs. (4)–(6) to determine the force magnitude (a) and phase (b). At low frequencies, the effective photothermal force is dominant, while at high frequencies, the radiation pressure force is dominant.

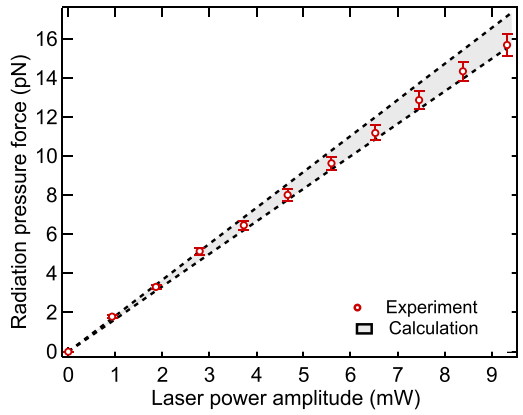

FIG. 4. Measured and calculated radiation pressure forces are in agreement within the experimental and calculated errors. The measured force corresponds to the peak value of the sinusoidal response in the time domain resulting from sinusoidal external illumination.

uncertainty in the fitting process and the precision of the Sader method in determining the spring constant.

In summary, we have performed quantitative measurements of radiation pressure in ambient conditions and found the experimental results to be in agreement with theory. The radiation pressure is much stronger than the effective photothermal forces when excitation occurs near the free end of a silicon nitride cantilever. Using a simple model, we identified and separated the radiation pressure and photothermal contributions. We envision this method as a practical technique to determine the response of optomechanical devices and as an additional method for cantilever spring constant calibration, if the incident laser power and the cantilever's optical reflectivity and absorptivity are known.[8] Further, we expect this technique to be an effective method for the study of optical forces on exotic metamaterials, which might be hindered by photothermal forces.[26–28]

This project was supported under a NASA Early Career Faculty Award (grant number NNX12AQ50G).

[1]J. C. Maxwell, *A Treatise on Electricity and Magnetism*, 1st ed. (Oxford University, 1873), p. 391.
[2]O. Marti, A. Ruf, M. Hipp, and H. Bielefeldt, Ultramicroscopy **42**, 345 (1992).
[3]D. R. Evans, P. Tayati, H. An, P. K. Lam, V. S. J. Craig, and T. J. Senden, Sci. Rep. **4**, 5567 (2014).
[4]D. Kleckner and D. Bouwmeester, Nature **444**, 75 (2006).
[5]S. Gigan, H. R. Böhm, M. Paternostro, F. Blaser, G. Langer, J. B. Hertzberg, K. C. Schwab, D. Bäuerle, M. Aspelmeyer, and A. Zeilinger, Nature **444**, 67 (2006).
[6]A. Schliesser, P. Del'Haye, N. Nooshi, K. J. Vahala, and T. J. Kippenberg, Phys. Rev. Lett. **97**, 243905 (2006).
[7]J. Chan, T. P. M. Alegre, A. H. Safavi-Naeini, J. T. Hill, A. Krause, S. Gröblacher, M. Aspelmeyer, and O. Painter, Nature **478**, 89 (2011).
[8]P. R. Wilkinson, G. A. Shaw, and J. R. Pratt, Appl. Phys. Lett. **102**, 184103 (2013).
[9]P. A. Williams, J. A. Hadler, R. Lee, F. C. Maring, and J. H. Lehman, Opt. Lett. **38**, 4248 (2013).
[10]Z. Marcet, Z. H. Hang, S. B. Wang, J. Ng, C. T. Chan, and H. B. Chan, Phys. Rev. Lett. **112**, 045504 (2014).
[11]U. Leonhardt, Nature **444**, 823 (2006).
[12]S. M. Barnett, Phys. Rev. Lett. **104**, 070401 (2010).
[13]M. Mansuripur, Opt. Commun. **283**, 1997 (2010).
[14]P. W. Milonni and R. W. Boyd, Adv. Opt. Photonics **2**, 519 (2010).
[15]C. H. Metzger and K. Karrai, Nature **432**, 1002 (2004).
[16]O. Hahtela and I. Tittonen, Appl. Phys. B **81**, 589 (2005).
[17]D. M. Weld and A. Kapitulnik, Appl. Phys. Lett. **89**, 164102 (2006).
[18]M. Allegrini, C. Ascoli, P. Baschieri, F. Dinelli, C. Frediani, A. Lio, and T. Mariani, Ultramicroscopy **42–44**, 371 (1992).
[19]N. Selden, C. Ngalande, S. Gimelshein, E. Muntz, A. Alexeenko, and A. Ketsdever, Phys. Rev. E **79**, 041201 (2009).
[20]B. Ilic, S. Krylov, and H. G. Craighead, J. Appl. Phys. **107**, 034311 (2010).
[21]M. Vassalli, V. Pini, and B. Tiribilli, Appl. Phys. Lett. **97**, 143105 (2010).
[22]J. E. Sader, J. W. M. Chon, and P. Mulvaney, Rev. Sci. Instrum. **70**, 3967 (1999).
[23]M. J. Higgins, R. Proksch, J. E. Sader, M. Polcik, S. Mc Endoo, J. P. Cleveland, and S. P. Jarvis, Rev. Sci. Instrum. **77**, 013701 (2006).
[24]S. Rast, C. Wattinger, U. Gysin, and E. Meyer, Rev. Sci. Instrum. **71**, 2772 (2000).
[25]S. M. Cook, K. M. Lang, K. M. Chynoweth, M. Wigton, R. W. Simmonds, and T. E. Schäffer, Nanotechnology **17**, 2135 (2006).
[26]J. Zhang, K. F. MacDonald, and N. I. Zheludev, Phys. Rev. B **85**, 205123 (2012).
[27]V. Ginis, P. Tassin, C. Soukoulis, and I. Veretennicoff, Phys. Rev. Lett. **110**, 057401 (2013).
[28]K. J. Chau and H. J. Lezec, Opt. Express **20**, 10138 (2012).